Available online at www.sciencedirect.com

ScienceDirect

Energy Procedia 74 (2015) 477 – 490

Energy Procedia

International Conference on Technologies and Materials for Renewable Energy, Environment and Sustainability, TMREES15

# Optimal Power Control Strategy of Maximizing Wind Energy Tracking and different operating conditions for Permanent Magnet Synchronous Generator Wind Farm

Youssef Errami[a,*], Mohammed Ouassaid[b], Mohamed Maaroufi[c]

[a]*Department of Physical – Faculty of Science- University Chouaib Doukkali, Eljadida, Morocco*
[b] *Department of Industrial Engineering, Ecole Nationale des Sciences Appliquées, Cadi Ayyad University, Safi, Morocco*
[c]*Department of Electrical Engineering, Mohammadia School's of Engineers, Mohammed V- Agdal University, Rabat, Morocco*

**Abstract**

This paper develops the model and the control of a Wind Farm System (WFS) based on Permanent Magnet Synchronous Generator (PMSG) and interconnected to the electric network. It evaluates the performance of the system for fault conditions as well as for normal working conditions. The proposed control law combines Vector Control (VC) and Maximum Power Point Tracking (MPPT) control methodology in order to maximize the generated power from Wind Turbine Generators (WTG). So, WFS can not only capture the maximum wind energy, but also can maintain the frequency and amplitude of the output voltage. Simulation results have shown the effectiveness of the proposed control method for variable speed WFS based on the PMSG.


Peer-review under responsibility of the Euro-Mediterranean Institute for Sustainable Development (EUMISD)

*Keywords:* WFS; PMSG; MPPT; Vector Control; Variable-speed control; Grid fault.

* Corresponding author. Tel.: 212-666185565.
*E-mail address: errami.emi@gmail.com*


Peer-review under responsibility of the Euro-Mediterranean Institute for Sustainable Development (EUMISD)
doi:10.1016/j.egypro.2015.07.732

## 1. Introduction

Recently, with technological advancement, wind power has grown rapidly and becomes the most competitive form of renewable energy resource [1-2]. Besides, Variable-Velocity Wind Energy Conversion Systems (VV-WECS) are the dominant technology in the present wind power industry for the reason that they possess several advantages, over the fixed speed systems, as the ability to obtain MPPT control methodology in order to extract maximum power at different wind, higher overall efficiency, power quality and it can be controlled to reduce aerodynamic noise and mechanical stress on VV-WECS by absorbing the wind-power fluctuations [3-4]. On the other hand, with the increased penetration of VV-WECS into power systems all over the world, WTG based on PMSG are becoming popular for variable-speed generation system and the use of the PMSG in large WTG is growing rapidly. It is connected directly to the turbine without gearbox and so it can operate at low speeds. Furthermore, it can reduce again weight, losses, costs, demands maintenance requirements [5-8] and, with the advance of power electronic technology, the wind farms are at present required to participate actively in electric network operation by an appropriate generation control methodologies [9-11]. In the literature, different controlling types of VV-WECS can be seen [12-16]. They use power electronics in combination with aerodynamic controls to regulate power, torque and velocity. Besides, the development in power electronics devices has further played an important role in the perfection of their controllability and reliability. Also, in the operation of the WTG, there is constantly the possibility of the faults for the system. One of the ordinary faults is short circuit. Thus, due to the increased number of VV-WECS connected to the electric network, instability of these systems and of the grid itself can occur.

In this context, this paper proposes a control strategy of PMSG wind energy generation system, and discusses back-to-back PWM converter control method. The block diagram of proposed VV-WECS is depicted in Fig. 1.

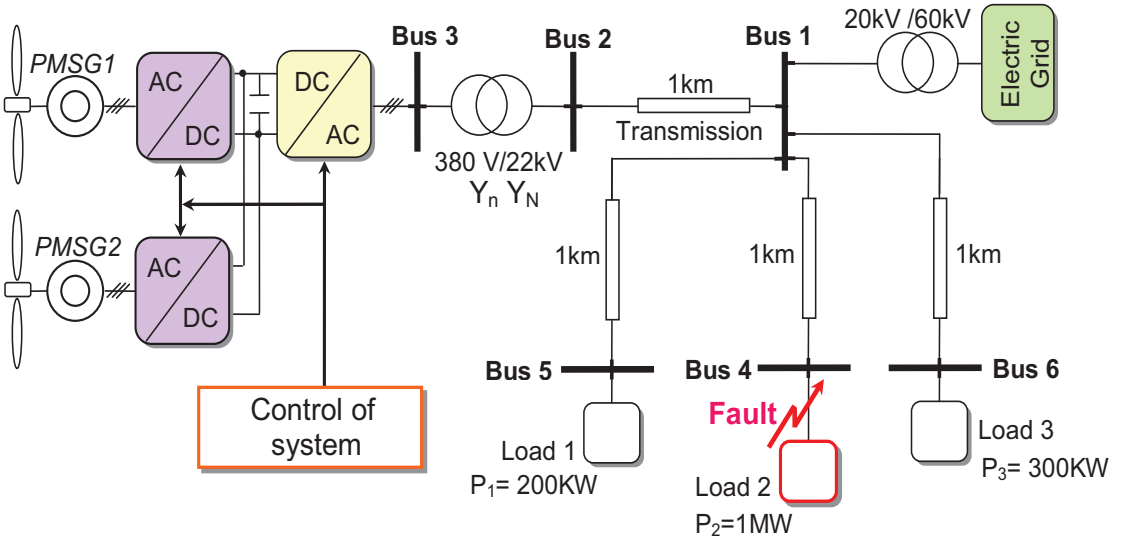


***Fig. 1.*** *Configuration of the system.*

The system model includes 2 PMSGs connected to a common DC-bus system. Each generator of the VV-WECS is connected to the DC-bus through a rectifier. The function of the grid-side converter is to maintain the DC-link voltage constant and to control the reactive and active power on the grid independently. The generator side rectifiers are used in order to track the maximum wind power. The proposed approach is based on a Vector Control theory (VC) for regulate of both grid-side and machine converters. So, the proposed control law combines Space Vector Modulation (SVM) and Maximum Power Point Tracking (MPPT) control strategy to maximize the generated power under varying wind speed and the grid fault condition. In addition, a pitch control scheme for variable velocity WTG is proposed in order to prevent WT damage from excessive wind speed.

The remainder of this paper is organized as follows. In Section 2, the models of the WTG and PMSG are developed. In Section 3, Vector Control (VC) of the system will be presented. The simulations results are presented and analyzed in Section 4. Finally, some conclusions are given in Section 5.

## 2. Modeling of WFS

### *2.1. Wind turbine characteristic*

A turbine generator can not fully capture wind energy. Then, the output power of the wind-turbine is described as [10]:

$$P_{Turbine} = \frac{1}{2}\rho\pi R^2 C_P(\lambda,\beta)v^3 \tag{1}$$

where, $\rho$ is the air density ( kg/m$^3$ ), $R$ is the blade radius (m), $C_P$ is the performance coefficient of the turbine which is a function of the pitch angle of rotor blades $\beta$ ( in degrees ) and $v$ is the wind speed (in m/s). The tip-speed ratio $\lambda$ is given by:

$$\lambda = \frac{\omega_m R}{v} \tag{2}$$

where $R$ and $\omega_m$ are the blade length (in m) and the wind turbine rotor speed (in rad/sec), respectively. The wind turbine mechanical torque output $T_m$ given as:

$$T_m = \frac{1}{2}\rho A C_P(\lambda,\beta)v^3 \frac{1}{\omega_m} \tag{3}$$

A generic equation is used to model the coefficient of power conversion $C_P(\lambda,\beta)$ based on the modelling turbine characteristics described in [7] as:

$$C_P = \frac{1}{2}\left(\frac{116}{\lambda_i} - 0.4\beta - 5\right)e^{-\left(\frac{21}{\lambda_i}\right)}$$
$$\frac{1}{\lambda_i} = \frac{1}{\lambda + 0.08\beta} - \frac{0.035}{\beta^3 + 1} \quad (4)$$

The coefficient of power conversion and so the power extracted are maximum at a certain value of tip speed ratio called optimum tip speed ratio $\lambda_{opt}$. Consequently, the maximum value of $C_P(\lambda,\beta)$, that is $C_{P_{\max}} = 0.41$, is achieved for $\lambda_{opt} = 8.1$ and for $\beta = 0^\circ$. Moreover, any change in the wind speed or the rotor velocity induces change in the tip speed ratio leading to power coefficient variation. Thus, the output power of the WTG is affected. This power is maximized at the particular rotational speed for various wind and it is obligatory to keep the rotor velocity at an optimum value of the tip speed ratio, $\lambda_{opt}$. As a result, the variable velocity WECS can operate at the peak of the $P(\omega_m)$ curve when the wind speed changes and the maximum power is extracted continuously from the wind (MPPT control) [17]. That is shown in Fig. 2.

### *2.2. Modelling of PMSG*

The mathematical model of a PMSG is usually defined in the rotating reference frame *d-q* as follows [18]:

$$v_{gd} = \left(R_g + pL_d\right)i_d - \omega_e L_q i_q \quad (5)$$

$$v_{gq} = \left(R_g + p.L_q\right).i_q + \omega_e L_d i_d + \omega_e \psi_f \quad (6)$$

where $v_{gq}$ and $v_{gd}$ are the quadrature stator and direct stator voltage, respectively. $i_q$ and $i_d$ are the quadrature stator and direct stator current, respectively. $R_g$ is the stator resistance, $L_q$ and $L_d$ are the inductances of the generator on the $q$ and $d$ axis, $\psi_f$ is the permanent magnetic flux and $\omega_e$ is the electrical rotating speed of the generator, defined by:

$$\omega_e = p_n \omega_m \quad (7)$$

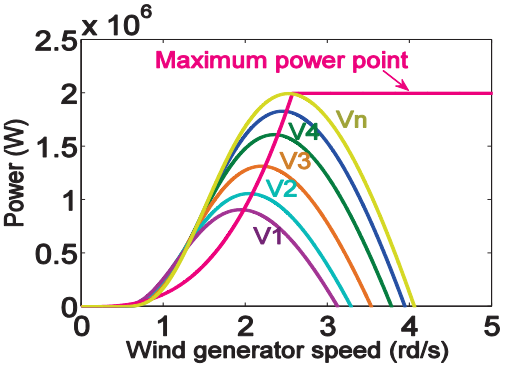


***Fig. 2.*** *Wind generator power curves at various wind speed*

where $p_n$ is the number of pole pairs of the generator and $\omega_m$ is the mechanical angular speed. The electromagnetic torque can be expressed as:

$$T_e = \frac{3}{2} p_n \left[ \psi_f i_q - \left( L_d - L_q \right) i_d i_q \right] \tag{8}$$

If $i_d = 0$ , the electromagnetic torque is described as:

$$T_e = \frac{3}{2} p_n \psi_f i_q \tag{9}$$

The dynamic equation of the wind turbine is given as:

$$J \frac{d\omega_m}{dt} = T_e - T_m - F\omega_m \tag{10}$$

where $T_m$ is the mechanical torque developed by the wind turbine, $F$ is the viscous friction coefficient and $J$ is the moment of inertia.

## 3. Control of system

### *3.1. Maximum Power Point Tracking (MPPT) and Pich Control*

The MPPT controller is used to generate the reference speed command which will enable the WTG to extract maximum power at different wind speeds. Thus, when the wind velocity changes, the speed of PMSG is controlled to follow the maximum power point trajectory and, the optimum rotational speed of the generator can be simply estimated as follows [17]:

$$\omega_{m-opt} = \frac{v\lambda_{opt}}{R} \tag{11}$$

The maximum extracted power of the WTG is given as:

$$P_{Turbine\_\max} = \frac{1}{2} \rho A C_{P\max} \left( \frac{R\omega_{m-opt}}{\lambda_{opt}} \right)^3 \tag{12}$$

As a result, the MPPT controller computes the optimum velocity of PMSG $\omega_{m-opt}$ and by regulating the WTG speed in different wind velocities the maximum power $P_{Turbine\_\max}$ is extracted. Also, if the wind speed reached the nominal value of WTG, the system of Pitch Angle controller enters in operation to prevent WT damage from excessive wind speed. Therefore, by reducing the coefficient $C_p$, both the power and rotor speed are maintained for above rated wind velocities. So, the blade pitch angle $\beta$, will increase until the wind turbine is at the rated speed. The implemented pitch angle system is shown in Fig. 3 where $P_{gm}$ is the generated power.

### *3.2. Control of the PMSG side converter with MPPT and Vector Control*

The generator-side converter is used to regulate the wind WTG, which enables optimal

velocity tracking for the optimal power capture from any particular wind speed. The proposed MPPT controller generates $\omega_{m-opt}$, the reference velocity of the PMSG, which when applied to the speed control loop of the generator side converter control system, maximum power will be produced by the WECS. Consequently, Vector Control (VC) is adopted and the control scheme shown in Fig. 4 is used as the control strategy for the generator side rectifier with double closed loop regulate. In the inside loop, the current controllers are used to regulate q-axis and d-axis stator current to follow the command, while a speed controller is used in the outside loop to regulate the generator speed so as to follow the command value $\omega_{m-opt}$, and produces corresponding q-axis current command $i_{qr}$. Also, $u_{sq}$ is obtained by the error of $i_{qr}$ and $i_q$ where $i_{qr}$ is the reference current.

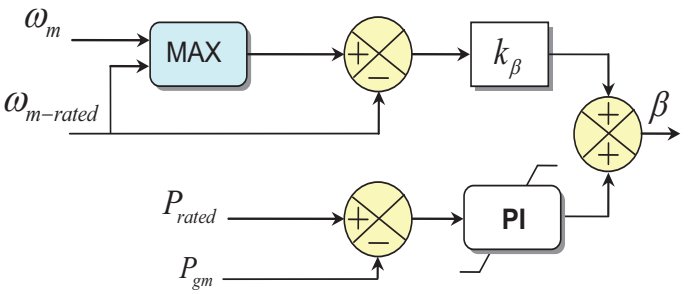


***Fig.3.*** *WECS Pitch angle controller*

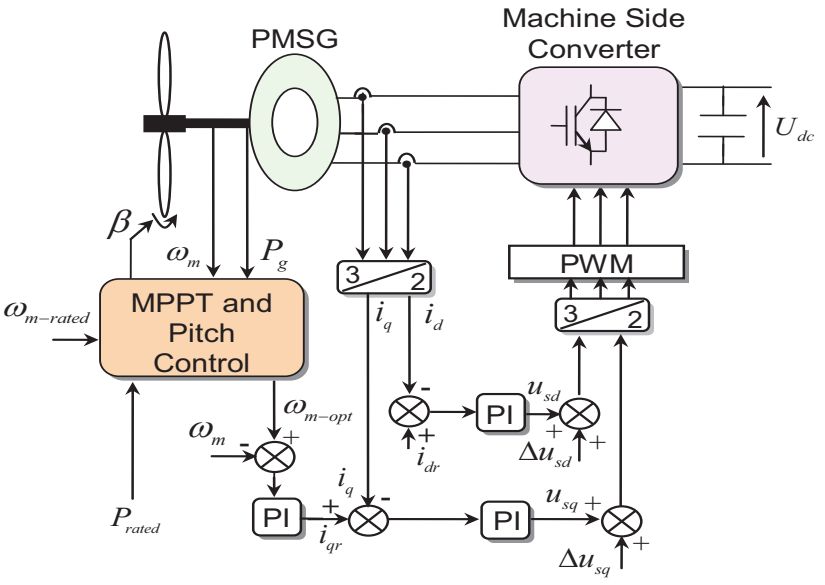


***Fig. 4.*** *Individual PMSG side converter control diagram.*

This error is delivered to a PI controller. In order to reduce the copper loss, the d-axis current component $i_{dr}$ is set to zero. Besides, voltage feed forward compensations, $\Delta u_{sq}$ and $\Delta u_{sd}$ are added into the control methodology so as to improve the dynamic response. Finally, we use PWM to produce the control signal to implement the vector control for the PMSG.

### *3.3. Grid Side Controller methodology*

The grid side converter is used to deliver the energy from the WTG side to the grid, to regulate the DC bus voltage, to adjust the quantity of the reactive and active powers delivered to the grid during wind variation in order to achieve Unity Power Factor (UPF) [13-16]. So, the Vector Control with two control loops is used. The implemented controller is depicted in Fig. 5. Then, in the inner control loops, PI controllers are used in order to regulate direct and quadrature current components, respectively. In addition, in the second loop, the DC-voltage controller stabilize, the DC voltage, by controlling the d-axis current with PI controller. The voltage balance across the inductor $L_f$ is given, in the rotating dq reference frame, by:

$$L_f \frac{di_{d-f}}{dt} = e_d - R_f i_{d-f} + \omega L_f i_{q-f} - v_d \tag{13}$$

$$L_f \frac{di_{q-f}}{dt} = e_q - R_f i_{q-f} - \omega L_f i_{d-f} - v_q \tag{14}$$

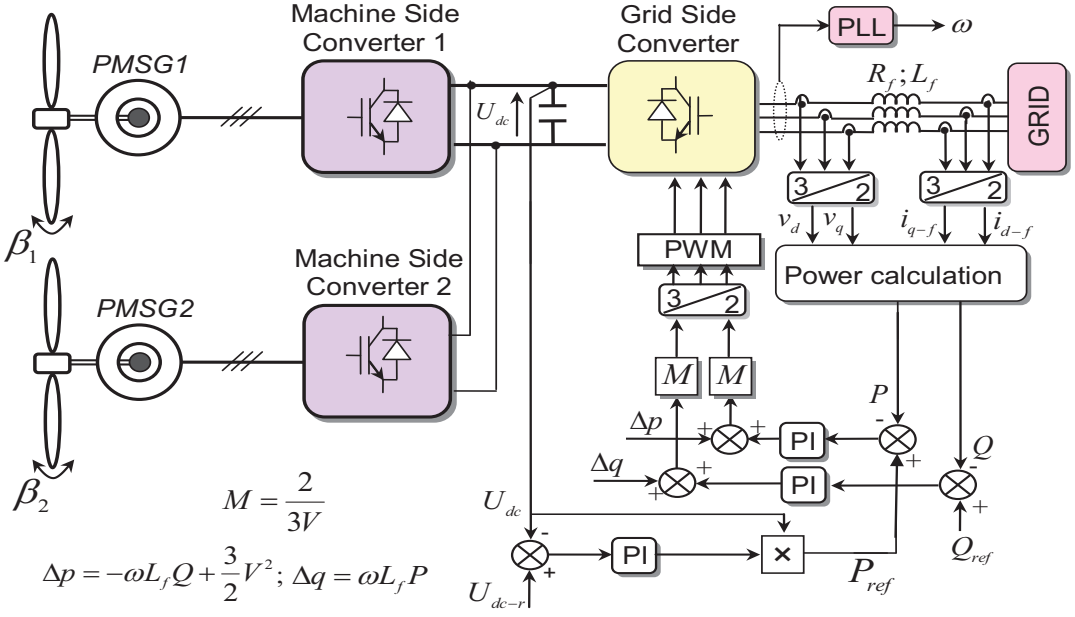


***Fig. 5.*** *Schematic of control strategy for VV-WECS.*

where $L_f$ and $R_f$ are the filter inductance and resistance respectively; $e_d$ and $e_q$ are the inverter d-axis q-axis voltage components respectively; $i_{d-f}$ and $i_{q-f}$ are the d-axis current and q- axis current of Grid. $v_d$ and $v_q$ are the grid voltage components in the d-axis q-axis voltage components respectively. The DC-side equation can be given by:

$$C\frac{dU_{dc}}{dt}=\frac{3}{2}(\frac{v_d}{U_{dc}}i_{d-f}+\frac{v_q}{U_{dc}}i_{q-f})-i_{dc} \tag{15}$$

where $i_{dc}$ and $U_{dc}$ are the grid side transmission line current and DC- bus voltage respectively. The instantaneous powers are given by:

$$Q=\frac{3}{2}(v_d i_{q-f}-v_q i_{d-f}) \tag{16}$$

$$P=\frac{3}{2}(v_d i_{d-f}+v_q i_{q-f}) \tag{17}$$

If the grid voltage space vector $\vec{u}$ is oriented on d-axis, then:

$$v_d=V \tag{18}$$

$$v_q=0 \tag{19}$$

So, equations (13-14) may be expressed as:

$$L_f\frac{di_{d-f}}{dt}=e_d-R_f i_{d-f}+\omega L_f i_{q-f}-V \tag{20}$$

$$L_f\frac{di_{q-f}}{dt}=e_q-R_f i_{q-f}-\omega L_f i_{d-f} \tag{21}$$

Then, the reactive power and active power can be expressed as:

$$Q=\frac{3}{2}Vi_{q-f} \tag{22}$$

$$P=\frac{3}{2}Vi_{d-f} \tag{23}$$

Therefore, according to the equation (20), (21), (22) and (23), $Q$ and $P$ are defined as the control variables, and the power control model can be expressed:

$$\frac{3}{2}Ve_d=R_f P+L_f\frac{dP}{dt}-\omega L_f Q+\frac{3}{2}V^2 \tag{24}$$

$$\frac{3}{2}Ve_q=R_f Q+L_f\frac{dQ}{dt}+\omega L_f P \tag{25}$$

Consequently, to provide decoupled control of active power and reactive power, the output power from the grid side converter, in the synchronous reference frame, could be formulated as:

$$\frac{3}{2}Ve_d = P_0 - \omega L_f Q + \frac{3}{2}V^2 \tag{26}$$

$$\frac{3}{2}Ve_q = Q_0 + \omega L_f P \tag{27}$$

Substitute (24) and (25) into (26) and (27), then:

$$R_f P + L_f \frac{dP}{dt} = P_0 \tag{28}$$

$$R_f Q + L_f \frac{dQ}{dt} = Q_0 \tag{29}$$

As a result, $Q_0$ and $P_0$ can be completed all the way through defining the power feedback loops as follows:

$$Q_0 = K_P(Q_{ref} - Q) + K_I \int (Q_{ref} - Q)dt \tag{30}$$

$$P_0 = K_P(P_{ref} - P) + K_I \int (P_{ref} - P)dt \tag{31}$$

Where $Q_{ref}$ and $P_{ref}$ are respectively rated active power and rated reactive power. $P_{ref}$ is used to maintain a constant output voltage and $Q_{ref}$ is determined by the power factor. We use the voltage regulator with PI control. So, rated active power $P_{ref}$ can be expressed as:

$$P_{ref} = U_{dc}(\dot{k}_p(U_{dc-r} - U_{dc}) + \dot{k}_I(\int (U_{dc-r} - U_{dc})dt)) \tag{32}$$

Fig. 5 illustrates the control block diagram of grid-side PWM inverter based on the above strategy. There are two closed-loops controls and PWM is used to produce the control signal in order to control the grid-side converter.

## 4. Simulation results

The complete VV-WECS with PMSG was simulated by Matlab/Simulink using the parameters given in Table 1. During the simulation, for the PMSG side converter control system, the d axis command current, $i_{dr}$, is set to zero; although, for the grid side inverter, $Q_{ref}$, is set to zero. On the other hand, the DC-link voltage reference is fixed at $U_{dc-r} = 1700V$ and the electric grid frequency value is steady at 50 Hz. The topology of the studied VV-WECS based on PMSG connected distribution network is depicted in Fig. 1, Fig. 4 and Fig.5. The grid voltage phase lock loop (PLL) system is implemented to track the fundamental phase and frequency. Fig. 6 illustrates the profile of wind velocities and rated wind speed considered in the simulation ($v_n$=12.4 m/s). Fig. 7 to Fig. 12 show the simulation results of pitch angles, coefficients of

power conversion $C_p$, tip speed ratio, rotor angular velocities and total power generated for system. So, for each turbine system, when the wind velocity increases, the rotor angular velocity increases proportionally too and the coefficient of power will drop to maintain the rated output power. $C_p$ is maintained to its maximum value ($C_{p\max}$ = 0.41) and the pitch angle is $\beta$ = 0°. The VV-WECS operates under MPPT control. In addition, the pitch angle variation is used to limit the rotor angular velocity. So, if the wind speed reaches the rated wind velocity of the turbine ($v_n$ =12.4 m/s), $C_p$ is decreasing because the operation of the pitch angle control is actuated and $\beta$ increases. Consequently, if the speed of wind continues to rise, rotational velocity and power extracted remains constant at the design limits. Fig. 11 depicts the optimum speed and the speed of PMSG1. It is seen that the speed of turbine follows the reference speed quite well. Fig. 13 illustrates the simulation result of dc link voltage that remains a constant value. Thus, this proves the effectiveness of the established regulators. Fig. 14 shows the variation and a closer observation of three phase current and voltage at Bus 3 (Fig. 1). Furthermore, the frequency is controlled and maintained at 50 Hz through a Phase Lock Loop (PLL) process. It is obvious that unity power factor of VV-WECS is achieved approximatively and is independent of the variation of the wind speed but only on the reactive power reference ($Q_{ref}$). On the other hand, in order to demonstrate the pertinence of the proposed approach, we test the performance of controller under short circuit fault. So, the fault event is a three-phase to ground short-circuit fault, at the Bus 4 of the 1 MW loads (Fig. 1). It is introduced at t = 6s for 200 ms. Fig. 15a-b and Fig. 15c show the waveforms of RMS lines ground voltages variations and a closer observation of three phase voltage at Bus 3 during the grid fault period. As illustrated, a three-phase grid short circuit fault at 6s forces the grid voltage to drop from 100% to 4% of its nominal values and the voltage dip lasts. After faults removed, the grid voltage recovers and the three voltages take their initial values. Fig. 16 shows the frequency performance. The maximum frequency deviation is 1.8 Hz and the frequency excursion is arrested after faults removed. It is obvious from Fig. 15d that the dc link voltage remains a constant value and the three phase voltage variations will not be transferred to the dc link voltage. Consequently, the dc link voltage has been controlled to enhance dynamic performance of the VV-WECS. The simulation results demonstrate that the control approach shows very good dynamic and steady state performance and works very well for VV-WECS based on the PMSG. In addition, the power is generated with the lowest possible impact in the electrical network frequency and voltage for fault conditions as well as for normal working conditions.

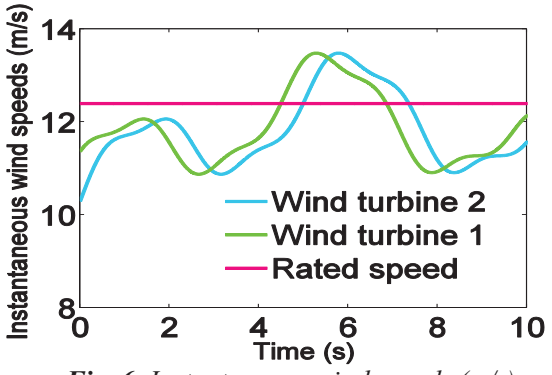


*Fig. 6. Instantaneous wind speeds (m/s)*

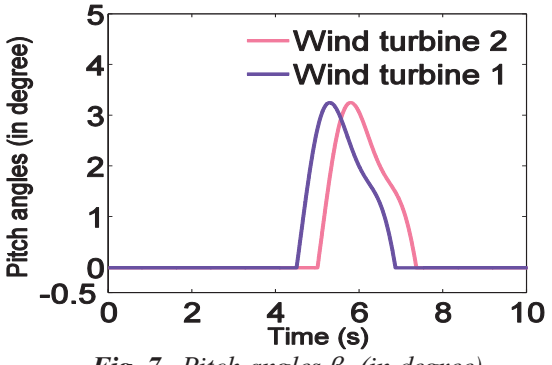


*Fig. 7. Pitch angles β (in degree).*

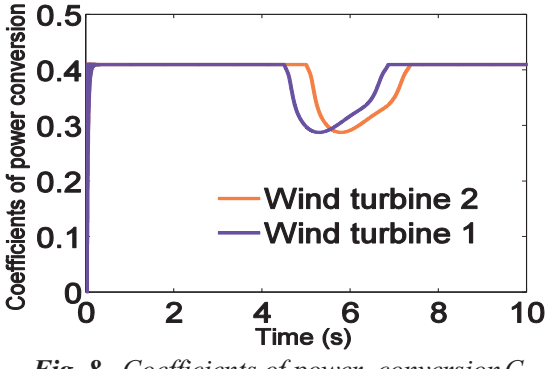


*Fig. 8. Coefficients of power conversion $C_p$.*

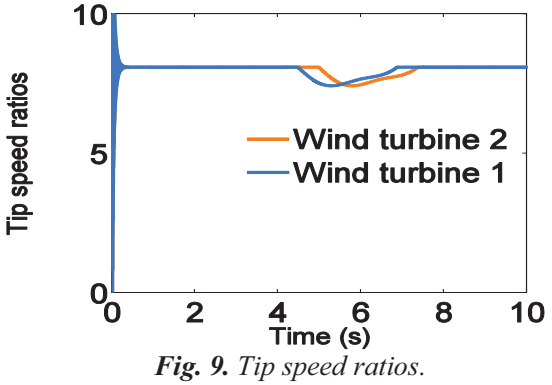


*Fig. 9. Tip speed ratios.*

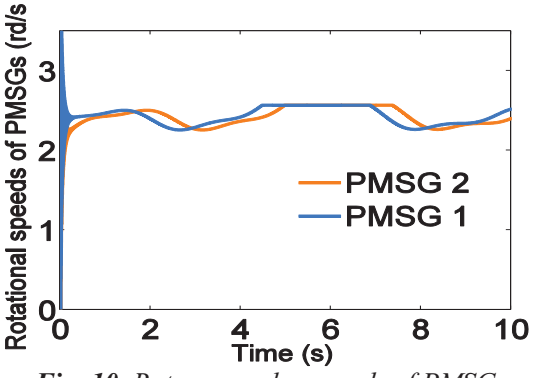


*Fig. 10. Rotors angular speeds of PMSGs.*

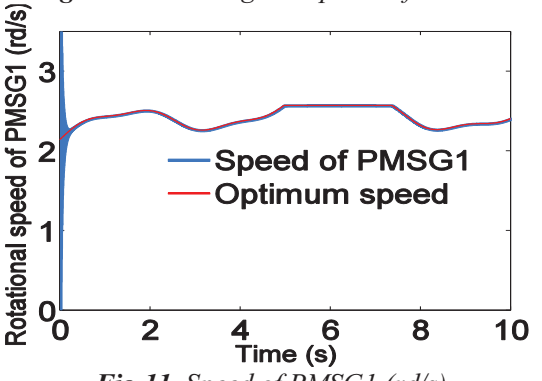


*Fig.11. Speed of PMSG1 (rd/s).*

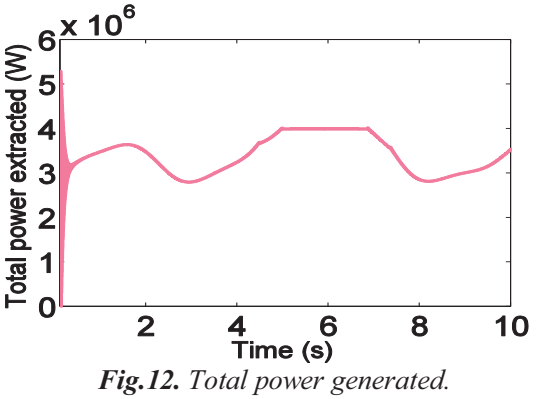


*Fig.12. Total power generated.*

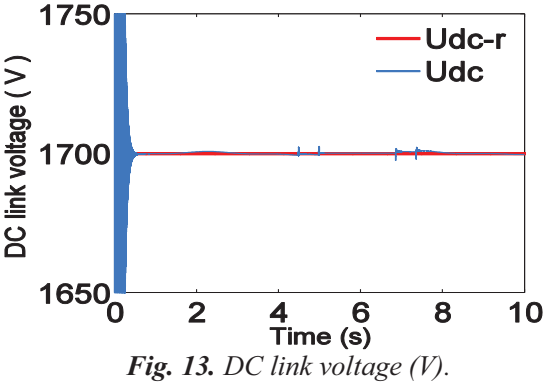


*Fig. 13. DC link voltage (V).*

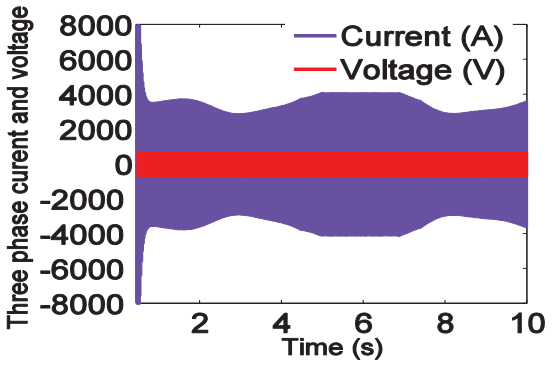


*a) Three phase current and voltage at Bus 3(V).*

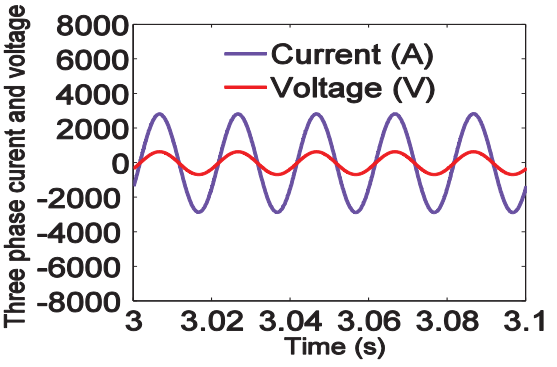


*(b) Closer observation of three phase current and voltage at Bus 3.*

***Fig. 14.*** *Three phase current and voltage at Bus 3.*

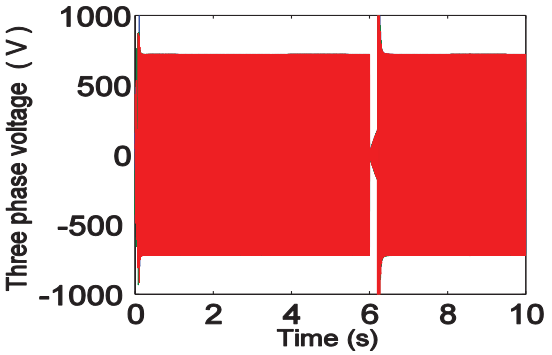


*(a) Three phase voltage at Bus 3 (V)*

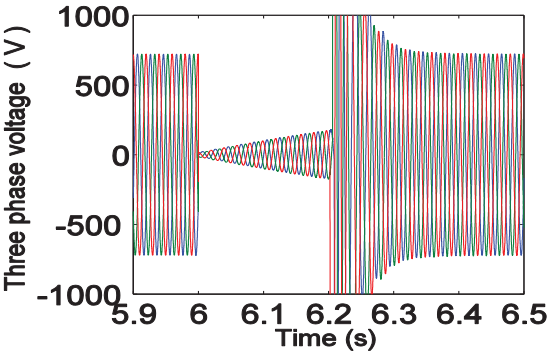


*(b) Closer observation of three phase voltage at Bus 3(V)*

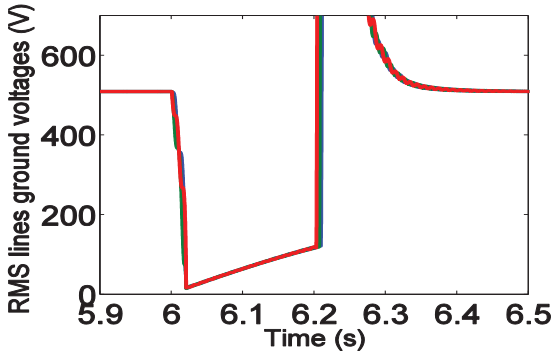


*(c) RMS lines ground voltages at Bus 3 (V)*

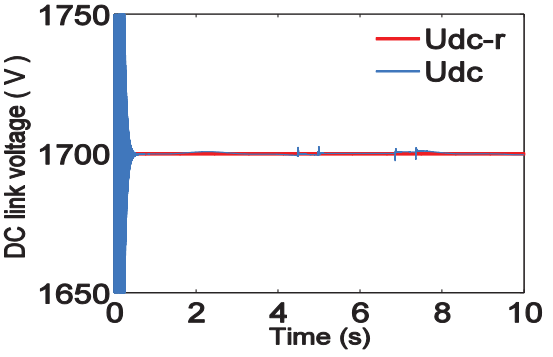


*(d) DC link voltage (V).*

***Fig. 15.*** *Performances of system under grid fault*

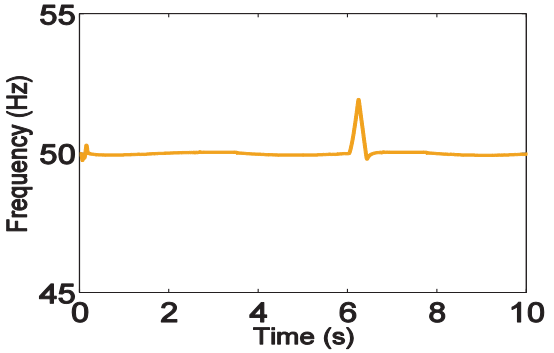


***Fig. 16.*** *Frequency performance at Bus 3 under grid fault (Hz)*

## 5. Conclusion

This paper deals with a control strategy of the VV-WECS based on the PMSG and connected distribution electrical network. A 4 MW PMSG variable speed wind power generation system is simulated to evaluate the performance of the proposed control strategy during the grid fault conditions as well as for normal working conditions. The control strategy can implement the theory of Maximum Power Point Tracking to adjust turbine velocity according to instantaneous wind speed and a pitch control scheme for VV-WECS to prevent wind turbine damage from excessive wind velocity. Moreover, control strategy based on VC theory is applied for generator converters and for inverters to implement the MPPT, DC link voltage regulation and unity power factor control under varying wind conditions. The simulations highlighted that the designed controllers show very good dynamic and steady state performance and works very well for VV-WECS based on the PMSG. Also, the power is generated with the lowest possible impact in the electrical network frequency and voltage for fault conditions as well as for normal working conditions.

Table 1

PARAMETERS OF THE POWER SYNCHRONOUS GENERATORS

| Parameter | Value |
|---|---|
| $P_r$ rated power | 2 (MW) |
| $\omega_m$ rated mechanical speed | 2.57 (rd/s) |
| $R$ stator resistance | 0.008( Ω ) |
| $L_s$ stator d-axis inductance | 0.0003 (H) |
| $\psi_f$ permanent magnet flux | 3.86 (wb) |
| $p_n$ pole pairs | 60 |

**References**

[1] Feifei Bu, Yuwen Hu, Wenxin Huang, Shenglun Zhuang, Kai Shi.Wide-Speed-Range-Operation Dual Stator-Winding Induction Generator DC Generating System for Wind Power Applications. IEEE Transactions On

Power Electronics, Vol. 30, No. 2, pp. 561-573, February 2015.
[2] Ye Wang, Herman Bayem, Maria Giralt-Devant, Vera Silva, Xavier Guillaud, Bruno Francois. Methods for Assessing Available Wind Primary Power Reserve. IEEE Transactions On Sustainable Energy, Vol. 6, No. 1, pp. 272- 280, January 2015.
[3] Kyung-Hyun Kim, Tan Luong Van, Dong-Choon Lee, Seung-Ho Song, Eel-Hwan Kim. Maximum Output Power Tracking Control in Variable-Speed Wind Turbine Systems Considering Rotor Inertial Power. IEEE Transactions On Industrial Electronics, Vol. 60, No. 8, pp. 3207-3217, August 2013.
[4] Y. Errami, M. Ouassaid, M. Maaroufi. Control scheme and maximum power point tracking of variable speed wind farm based on the PMSG for utility network connection. IEEE-International Conference on Complex Systems (ICCS'12), pp.1–6, November 2012**.**
[5] Salvador Alepuz, Alejandro Calle, Sergio Busquets-Monge, Samir Kouro, Bin Wu. Use of Stored Energy in PMSG Rotor Inertia for Low-Voltage Ride-Through in Back-to-Back NPC Converter-Based Wind Power Systems. IEEE Transactions On Industrial Electronics, Vol. 60, No. 5, pp. 1787-1796, May 2013 .
[6] Natalia Angela Orlando, Marco Liserre, Rosa Anna Mastromauro, Antonio Dell'Aquila. A Survey of Control Issues in PMSG-Based Small Wind-Turbine Systems. IEEE Transactions On Industrial Informatics, Vol. 9, No. 3, pp. 1211-1221 August 2013.
[7] Y.Errami, M.Hilal M.Benchagra, M.Ouassaid, M.Maaroufi. Nonlinear Control of MPPT and Grid Connected for Variable Speed Wind Energy Conversion System Based on the PMSG. Journal of Theoretical and Applied Information Technology, Vol. 39, No.2, pp.205- 217, May 2012.
[8] Changliang Xia, Zhiqiang Wang, Tingna Shi, Zhanfeng Song. A Novel Cascaded Boost Chopper for the Wind Energy Conversion System Based on the Permanent Magnet Synchronous Generator. IEEE Transactions On Energy Conversion, Vol. 28, No. 3, pp. 512- 522, September 2013.
[9] Nuno M. A. Freire, Jorge O. Estima, António J. Marques Cardoso. A New Approach for Current Sensor Fault Diagnosis in PMSG Drives for Wind Energy Conversion Systems. IEEE Transactions On Industry Applications, Vol. 50, No. 2, pp. 1206-1214, March/April 2014.
[10] Eduardo Giraldo, Alejandro Garces. An Adaptive Control Strategy for a Wind Energy Conversion System Based on PWM-CSC and PMSG. IEEE Transactions On Power Systems, Vol. 29, No. 3, pp. 1446-1453, May 2014.
[11] Marius Fatu, Frede Blaabjerg, Ion Boldea. Grid to Standalone Transition Motion Sensorless Dual-Inverter Control of PMSG With Asymmetrical Grid Voltage Sags and Harmonics Filtering. IEEE Transactions On Powers Electronics, Vol. 29, No. 7, pp. 3463-3472, July 2014.
[12] Dante Fernando Recalde Melo, Le-Ren Chang-Chien. Synergistic Control Between Hydrogen Storage System and Offshore Wind Farm for Grid Operation. IEEE Transactions On Sustainable Energy, Vol. 5, No. 1, pp. 18-27, January 2014.
[13] Venkata Yaramasu, Bin Wu, Salvador Alepuz, Samir Kouro. Predictive Control for Low Voltage Ride Through Enhancement of Three-Level Boost and NPC Converter Based PMSG Wind Turbine. IEEE Transactions On Industrial Electronics, Vol. pp, No. 99, pp. 1-12, March 2014.
[14] Y. Errami, M. Maaroufi, M. Ouassaid. A MPPT vector control of electric network connected wind energy conversion system employing PM synchronous generator. IEEE International Renewable and Sustainable Energy Conference (IRSEC), pp. 228–233,2013.
[15] Jiawei Chen, Jie Chen, Chunying Gong. On Optimizing the Aerodynamic Load Acting on the Turbine Shaft of PMSG-Based Direct-Drive Wind Energy Conversion System. IEEE Transactions On Industrial Electronics, Vol. 61, No. 8, pp. 4022-4031, August 2014.
[16] Nuno M. A. Freire, António J. Marques Cardoso. Fault-Tolerant PMSG Drive With Reduced DC-Link Ratings for Wind Turbine Applications. IEEE Journal Of Emerging And Selected Topics In Power Electronics, Vol. 2, No. 1, pp. 26- 34, March 2014.
[17] Giampaolo Buticchi, Emilio Lorenzani, Member, Fabio Immovilli, Claudio Bianchini. Active Rectifier With Integrated System Control for Micro wind Power Systems. IEEE Transactions On Sustainable Energy, Vol. 6, No. 1, pp. 1-10, January 2015.
[18] Y.Errami, M.Hilal, M.Benchagra, M.Maaroufi, M.Ouassaid. Nonlinear control of MPPT and grid connected for wind power generation systems based on the PMSG. 2012 International Conference on Multimedia Computing and Systems (ICMCS), pp.1055-1060, May 2012.